Effects of external global noise on the catalytic CO oxidation on Pt(110)

P. S. Bodega,[1] S. Alonso,[1,2] and H. H. Rotermund[3,a)]
[1]*Fritz-Haber Institute of the Max Planck Society, Faradayweg 4-6, 14195 Berlin, Germany*
[2]*Physikalisch-Technische Bundesanstalt, Abbestrasse 2-12, 10587 Berlin, Germany*
[3]*Department of Physics and Atmospheric Science, Dalhousie University, Halifax, Nova Scotia B3H 3J5, Canada*

(Received 14 May 2008; accepted 12 January 2009; published online 26 February 2009)

Oxidation reaction of CO on a single platinum crystal is a reaction-diffusion system that may exhibit bistable, excitable, and oscillatory behavior. We studied the effect of a stochastic signal artificially introduced into the system through the partial pressure of CO. First, the external signal is employed as a turbulence suppression tool, and second, it modifies the boundaries in the bistable transition between the CO and oxygen covered phases. Experiments using photoemission electron microscopy together with numerical simulations performed with the Krischer–Eiswirth–Ertl model are presented. © *2009 American Institute of Physics*. [DOI: 10.1063/1.3078037]

I. INTRODUCTION

Chemical reactions in extended media are one of the characteristic systems where pattern formation outside equilibrium can be observed. The nonlinearity of such reactions and the diffusion of its components induce the formation of complex patterns. The Belousov–Zhabotinsky reaction and the catalytic oxidation of CO on single crystal platinum surfaces are chemical examples where spiral waves, target patterns, or chemical turbulence have been studied.[1] Such systems have been extensively employed because it is relatively easy to control the chemical and physical conditions which are responsible for the formation of the spatiotemporal structures.[2]

Natural systems are unavoidably subject to random fluctuations (noise), stemming from either environmental variability or thermal effects. These undesirable perturbations mask and affect the deterministic dynamics of the system. Such fluctuations gain importance far from equilibrium[3,4] because they can interact with the nonlinearities of the system, giving rise to a rich variety of behaviors.[5] The effects of noise in extended active media[6] are particularly interesting. Chemical reactions are one of the most convenient systems used to study this type of phenomenology. Both Belousov–Zhabotinsky and chlorine dioxide–iodine–malonic acid reactions are good examples where the effects of noise have been studied extensively. The photosensitive version of such reactions is particularly suitable for the introduction of controlled external fluctuations through a stochastic illumination,[7–9] where the characteristic time and length can be easily tuned by a computer. The most significant results have been obtained for noises with spatial structure. However, interesting results have also been observed with homogeneous noisy illumination[10] or applying a stochastic electric field.[11]

Heterogeneous catalytic CO oxidation is well known for the wealth of variety of pattern formations that can develop on the surface of a single crystal. Depending on the partial pressure of the species inside the reactor chamber, different types of patterns have been observed: Spiral waves, target patterns, standing waves, and turbulence.[12] This reaction is not photosensitive but the pressure of the reactants can be externally controlled;[13] in particular, a stochastic signal can be artificially introduced. There is no spatial structure in the external signal and therefore the noise is homogeneous. Previous experimental and analytical studies on bistable reactions show how noise can anticipate the transitions between both bistable states in CO oxidation in Ir(111),[14,15] and how local fluctuations become important.[16] Theoretical predictions of stochastic resonance in the catalytic oxidation of CO in Pt(110) have also been reported.[17]

The effects of external noise can be interpreted as a control mechanism of the different types of patterns, and by tuning the characteristics of these external fluctuations, transitions and new states can be achieved. The control of chemical turbulence is a problem tackled from a number of different angles.[2,18] In the CO–Pt system, for instance, attempts have been made with feedback techniques,[19,20] local control,[21] periodical global forcing,[22] and resonant global forcing.[13]

Two different scenarios of noise effects are considered here: First, we study the elimination of turbulence through stochastic forcing, and second, we focus on the noise related modification of the boundaries in the bistable transition between the CO and oxygen covered phases. Both experimental studies are contrasted with the results of numerical simulations performed with the Krischer–Eiswirth–Ertl (KEE) model for the CO oxidation in Pt(110).[23] Finally, we discuss the results and compare them with previous control strategies for the catalytic CO oxidation.

II. EXPERIMENTAL SETUP

To perform the experiments, a single crystal Pt(110) is mounted inside a constant flux ultrahigh vacuum (UHV) chamber, where CO and oxygen are constantly added into, while the total pressure is kept constant by continuously

a)Author to whom correspondence should be addressed. Electronic mail: harm.rotermund@dal.ca.

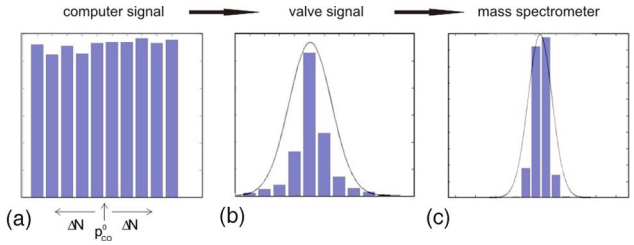

FIG. 1. (Color online) Histograms of the $p_{CO}(t)$. (a) Generated signal, (b) signal in the dosing system, and (c) mass spectrometer signal inside the reaction chamber (Gaussian distribution overplotted).

pumping the entire system. A photoemission electron microscopy (PEEM) (Ref. 24) allows us to spatially resolve the local work function of the adsorbate species and to record it with a charge coupled device camera at a rate of 25 full frames/s. A meaningful modulation of the CO partial pressure was introduced into the system as a computer controlled source of random fluctuations following:

$$p_{CO}(t_i) = p_{CO}(1 + \psi_i \cdot \Delta N), \tag{1}$$

where ψ_i is a random number between −1 and +1 that is regenerated by the computer in time intervals of Δt ($t_i - t_{i-1} = \Delta t$). ΔN is the percentage of CO partial pressure that is added to the base value. The combination of the parameters Δt and ΔN determines how fast and how much $p_{CO}(t)$ changes, or in other words, the magnitude of the multiplicative noise present in the reaction. The two parameters are then used by the computer to control the CO gas dosing valve. Due to the solenoid valve effective reaction time, and the low pass filtering between the dosing system and the chamber, the generated rectangular signal is integrated by the system, resulting in a Gaussian-type distribution in the solenoid valve and in the reaction chamber, as shown in Fig. 1. Hence, the CO partial pressure in the reaction environment has a fluctuating value between $p^0_{CO} + \Delta N$ and $p^0_{CO} - \Delta N$, homogeneous in space, characterized by a histogram like the one depicted in Fig. 1(b), which resembles a Gaussian noise.

III. REACTION MODEL

In this work we use the KEE model,[23] which has been previously employed to study CO oxidation in surfaces of Pt(110).[25,26] The model consists of three coupled equations for the CO and oxygen coverage, respectively, u and v, and the fraction of the surface found in the nonreconstructed Pt 1×1 phase, corresponding to the third variable w. The equations read as

$$\partial_t u = D\nabla^2 u + k_1 s_{CO} p_{CO}(1 - u^3) - k_2 u - k_3 uv, \tag{2}$$

$$\partial_t v = k_4 p_{O_2}[s_{O,1\times1} w + s_{O,1\times2}(1 - w)](1 - u - v)^2 - k_3 uv, \tag{3}$$

$$\partial_t w = k_5 \left(\frac{1}{1 + \exp\left(\frac{u_0 - u}{\delta u} \right)} - w \right). \tag{4}$$

For a brief explanation of the model and the parameter values used here, see Table I. Such parameters correspond to previous numerical studies of the same experimental system under similar conditions.[25] The values of the partial pressures of CO and oxygen are, respectively p_{CO} and p_{O_2}, and they are specified for each case studied here. Several variants of this model have been previously employed to study different types of bifurcations observed in the CO oxidation or the dynamics of spiral waves.[27] The effect of the temperature can also be considered, assuming an Arrhenius-type dependence on the temperature of the model parameters.[26] Here, we keep the parameter corresponding to the temperature constant $T = 542.35$ K.

The phase diagram of the KEE model for both partial pressures (p_{CO} and p_{O_2}), keeping the rest of the parameters constant, is shown in Fig. 2. It corresponds to the system without diffusion, thus there is no information about spatial patterns. As expected for large values of the pressure of oxygen and low pressure of CO, the oxygen covered phase is stable. On the other hand, for large values of the pressure of CO and low pressure of oxygen, the CO covered phase is also stable. For intermediate values of both partial pressures (typically with the pressure of oxygen three times larger than the pressure of CO), both phases compete. While for large pressures, this competition gives rise to bistability and hysteresis, for intermediate pressures it also induces oscillations. In this region of periodic alternance not only global oscillations but also turbulence are observed depending on the values of the parameters. For low pressures of both CO and oxygen, a continuous transition between both phases is ob-

TABLE I. Parameters of the reaction model.

Parameter	Value	Meaning
k_1	3.14×10^5 mbar^{-1}	Impingement rate of CO
k_2	10.21 s^{-1}	CO desorption rate
k_3	283.8 s^{-1}	CO Reaction rate
k_4	5.86×10^5 s^{-1} mbar^{-1}	Impingement rate of O_2
k_5	1.6 s^{-1}	Phase transition rate
s_{CO}	1.0	CO sticking coefficient
$s_{O_{1\times1}}$	0.6	Oxygen sticking coefficient on the 1×1 phase
$s_{O_{1\times2}}$	0.4	Oxygen sticking coefficient on the 1×2 phase
u_0, δ_u	0.35, 0.05	Parameters for the structural phase transition
D	40 μm s^{-1}	CO diffusion coefficient
u_{ref}	0.3358	Reference CO coverage

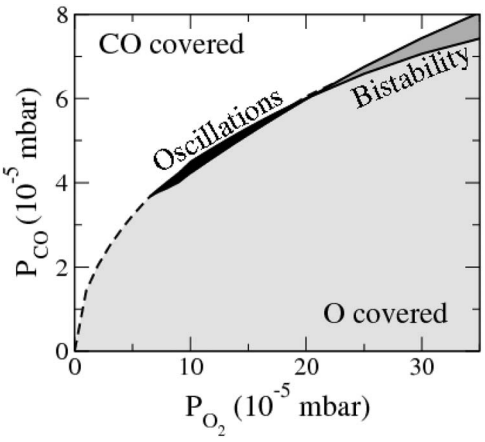

FIG. 2. Phase diagram of the KEE model keeping the values of Table I constant. This diagram does not take into account the diffusion. Regions of oscillations and bistability are marked as black and dark gray areas, respectively.

served (dashed line in Fig. 2). This diagram qualitatively agrees with the experiments of CO oxidation on Pt(110).

In order to mimic the experimental conditions of random external modulations of the partial pressure of CO, we add a stochastic variable to the value of the pressure,

$$p_{CO} = p^0_{CO}(1 + \xi_e(t)), \tag{5}$$

where the variable $\xi_e(t)$ is a Gaussian spatially homogeneous white noise with null mean $\langle \xi_e(t) \rangle = 0$ and variance $\langle \xi_e(t)\xi_e(t') \rangle = 2\sigma^2\delta(t-t')$, where σ^2 is the intensity of the noise.

It is known that the surface of the crystal is not completely homogeneous and there are heterogeneities, which affect the propagation of the surface waves qualitatively. Such heterogeneities are consequence of several experimental factors (facetting, subsurface species, or crystal surface defects) and their activity may depend on several processes such as the local concentration of CO and O in an unknown way. In order to consider these internal fluctuations, we introduce an additive noise term $\xi_i(x,t)$ in the first equation of the model equation (2). This variable is Gaussian white noise, distributed in space with null mean $\langle \xi_i(x,t) \rangle = 0$ and variance $\langle \xi_i(x,t)\xi_i(x',t') \rangle = 2\epsilon_i\delta(x,x')\delta(t-t')$, where ϵ_i is the intensity of the noise. We note that these internal fluctuations are not related to the external experimental noise, which has been introduced above as multiplicative noise. Since we are not going to do a systematic study of these internal fluctuations, we are keeping the intensity of this noise low and constant ($\epsilon_i = 0.0005$) for all of the numerical simulations following. They will act as precursors in the simulations during transitions.

In summary, we introduce two types of random processes: First, a homogeneous random noise through the parameter p_{CO}, mimicking the external experimental noise introduced by the CO pressure, which is the main object of study in this paper. Second, a spatiotemporal noise that takes into account different experimental sources of randomness.

We integrate Eqs. (2)–(4) using a finite differences scheme and the Heun method[28] for stochastic partial differential equations. Two-dimensional (2D) numerical simulations are completed using a finite differences scheme with a spatial and temporal discretization of $\delta x = 2\ \mu$m and $\delta t = 0.001$ s, respectively. We employ periodic boundary conditions in all of the simulations.

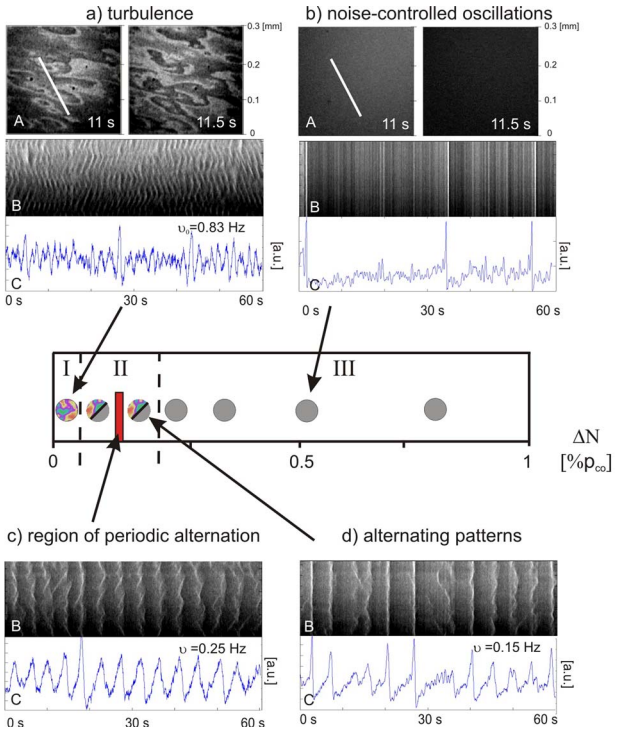

FIG. 3. (Color online) PEEM snapshots A of the platinum surface and space-time plots B, for different values of ΔN applied on an initial turbulence state of the chemical reaction. The space-time plots represent the reaction pattern development in time along the white bar depicted on A. The corresponding pixel image intensities are plotted on C. Reaction parameters are $T = 540$ K, $p_{O_2} = 1.3 \times 10^{-4}$ mbar, $p^0_{CO} = 6.6 \times 10^{-5}$ mbar, and $\Delta t = 0.5$ s. Three regime differentiated areas are pointed out (I, II, and III), showing (a) turbulence, (b) noise-controlled oscillations, (c) periodic alternation, and (d) alternating patterns, which are further commented on in the text.

IV. TURBULENCE SUPPRESSED BY NOISE

Spatiotemporal chemical turbulence spontaneously develops on a platinum crystal surface for a window of values of the reaction parameters (reactants, partial pressures, and temperature). Such turbulence is characterized by the continuous creation and annihilation of phase defects on the surface.[29] Although it corresponds to a complex state, a characteristic frequency can still be obtained. Such turbulence can be effectively suppressed by a noise modulation of the reactants, namely, $p_{CO}(t)$.

Figure 3 represents the corresponding spatiotemporal patterns seen when different noise intensities are applied to a turbulent regime. In the absence of external noise, spiral turbulence develops freely [see 2D images in Fig. 3(a)]. For large intensities of the fluctuations (above 0.2% p_{CO}), the noise completely annihilates the reaction dynamics; the whole system then follows the noisy signal [Fig. 3(b)]. For intermediate noise intensity, the system is driven to a partially suppressed state featuring an alternation between asynchronized and homogeneous global oscillations [Fig. 3(d)]. It corresponds to a competition between the turbulence behavior of the surface and the global synchronization produced by

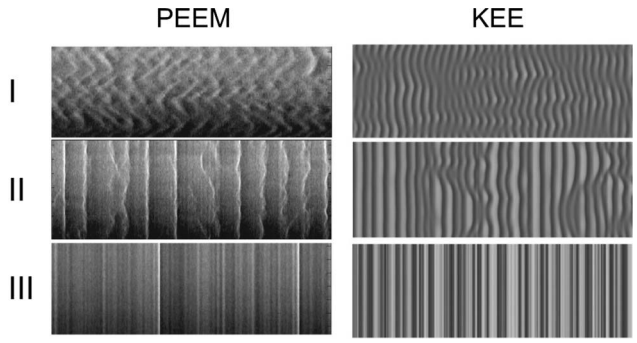

FIG. 4. Compared space-time plots corresponding to the turbulence suppression map regions I, II, and III; experiments (PEEM) vs simulations (KEE). Simulations are performed with the values of the partial pressures: $p_{O_2}=1.3\times10^{-4}$ mbar and $p^0_{CO}=4\times10^{-5}$ mbar in a system of size 0.2×0.2 mm^2. From top to bottom, the corresponding noise intensities are $\sigma=0.0\%\ p^0_{CO}$, $\sigma=0.25\%\ p^0_{CO}$, and $\sigma=2.5\%\ p^0_{CO}$.

the noise. This alternation was observed to be regular and periodic for a particular range of parameters [Fig. 3(c)]. Remarkably, the frequency of such responses are different than the characteristic frequency of the spiral turbulence. Finally, noise reaches values that completely annihilate the reaction dynamics; the system then follows the noisy signal.

The natural frequency of the system is affected by the noise. Figure 3 shows how the periodicity of the local oscillations changes with ΔN visible within the snapshots and the space-time plots, and compares the initial spiral turbulence of region I with the periodic induced patterns within region II, with the noise-controlled region III for a particular fixed value of Δt. Region III has no local periodicity whatsoever and reflexes the imposed random oscillations.

Region II in Fig. 3 encompasses the range of noise parameters in which the original spiral turbulence is not completely suppressed. Interaction with noise drives the active media through transient states, alternating between spatiotemporal chaos and a lack of patterns. Furthermore, for certain parameters these cycles may become regular. At the bottom left of Fig. 3, suppressed patterns alternating with reactivated turbulence in regular cycles of 4 s can be seen. The noise parameters corresponding to this induced behavior draw a narrow stripe in the turbulence suppression map (seen red bar in Fig. 3). Along that stripe, the interplay between excitability, refractory time, noise, and diffusion results in time regularity.

Larger or faster modulations than those showed in Fig. 3 are not considered here because of the limitations of the experimental setup (experiments showed strong disagreement between the computer values and the real state in the chamber for values $\Delta t<0.1$ or $\Delta N>3\%\ p^0_{CO}$). Therefore this study project was specifically focused on the smallest fluctuations with a relevant impact.

The series of space-time plots depicted in Fig. 4 shows the typical surface dynamics of the three regions (I, II, and III) addressed in Fig. 3 compared with numerical simulations; one can see that the plots based on the KEE model qualitatively agree with the experimental results. Wave turbulence (I), alternation of global oscillations and wave turbulence (II), and dominance of the noise (III) are observed in both cases.

The results of the numerical simulations agree and confirm the experimental results. Under parameter values corresponding to turbulence in the KEE model, the introduction of a global stochastic signal may induce the global coordinating of the whole system. For intermediate values of the external signal, a competition of the global coupling and the deterministic turbulent dynamics is observed, giving rise to intermittent turbulence and a number of intermediate patterns. For some noise intensities, periodic oscillations are observed and even standing waves or pacemakers are temporarily created by the global noise.

In the numerical simulations, the frequency of the spatiotemporal patterns also decreases with the noise intensity. The patterns of the chemical turbulence can be characterized by large frequencies. The global noise not only couples the whole system but also reduces the frequency of the patterns.

V. TRANSITIONS ANTICIPATED BY NOISE

Further experiments were focused on the bistable transition from a mainly oxygen covered Pt crystal to a mainly CO covered state. These experiments start with a certain amount of oxygen in the reaction chamber ($p_{O_2}=1.1\times10^{-4}$ mbar) with no CO. Once the surface is oxygen covered, the p_{O_2} is kept constant and then the p_{CO} is increased while adding additional fluctuations to it. For a large enough CO partial pressure, all of the adsorbed oxygen reacts away releasing CO_2, the sample is completely CO covered and the transition is complete. This process is clearly discernible in the PEEM images (top of Fig. 5): It is seen as the change from a uniform dark area to a uniformly bright one through a number

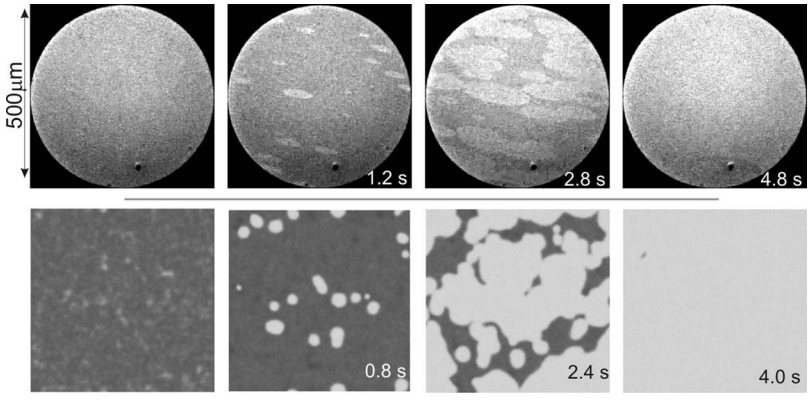

FIG. 5. PEEM snapshots (top) compared with numerically generated images (bottom). Different stages of the bistable transition, oxygen covered to CO covered can be seen. Experimental parameters are $T=509$ K, $p_{O_2}=1.1\times10^{-4}$ mbar, $\Delta t=0.25$ s, and $\Delta N=0.5\%\ p^0_{CO}$. Parameters used for the simulation are $p_{O_2}=4.5\times10^{-4}$, $p_{CO}=9.08\times10^{-5}$ in a system of size 0.4×0.4 mm^2, and internal noise $\epsilon_i=0.0005$.

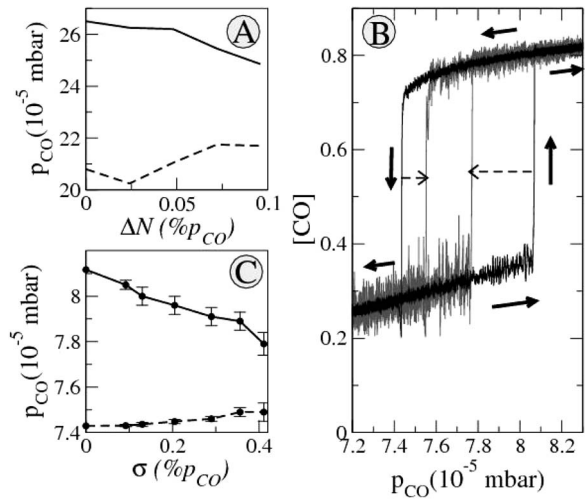

FIG. 6. Panel (a) shows the critical p_{CO} of both transitions, from oxygen covered to CO covered (solid line) and from CO covered to oxygen covered platinum (dashed line), for a value of applied noise. Reaction parameters are $T=509$ K, $p_{O_2}=1.1\times10^{-4}$ mbar, and $\Delta t=0.1$ s. Panel (b) shows the hysteresis loop for two noise intensities $\sigma=0.09\%$ p_{CO} and $\sigma=0.28\%$ p_{CO}. Panel (c) represents the corresponding numerical simulation plotted in terms of the simulation parameter σ. Numerical simulations have been completed with $p_{O_2}=3.5\times10^{-4}$ mbar in a system of 0.2×0.2 mm^2.

of growing bubbles. Due to the introduction of the additive noise in Eq. (2), the KEE model casts similar transition patterns (bottom of Fig. 5). The intensity of such additive noise has been tuned to qualitatively reproduce the experimental patterns shown in Fig. 5 and kept constant for all of the simulations. Without such noise, the system basically behaves homogeneously and no bubbles would be observed.

The same steps are followed backward for the backtransition to the initial CO covered state. Nevertheless, the critical p_{CO} is lower in this case, which is explained by the asymmetric inhibition of the reaction: The oxygen covered Pt does not behave in the same way as the poisoned CO covered surface.[30] There is an inherent hysteresis loop in this bistable transition due to the asymmetry of the reaction. Figure 6(a) describes how the mentioned hysteresis loop shrinks as the noise applied is larger.

Equivalent numerical simulations in the bistable region reproduce the main features of the hysteresis loop observed in the experiments. Starting from an oxygen covered phase, the pressure of CO is slowly increased inducing the transition to the CO covered phase. The posterior reduction of the CO pressure shows a lower value for the transition, giving rise to the hysteresis loop. Two numerical realizations with different noise intensities of this loop are shown together in Fig. 6(b). Larger noise intensities imply smaller hysteresis loops. This reduction in the size of the loop is plotted in Fig. 6(c).

VI. DISCUSSION

When the CO oxidation on Pt system shows spiral turbulence and global noise is introduced, this noise behaves as an overall coordinating factor that introduces a certain spatial coherence to otherwise spatially discoordinated oscillations. In this way, chemical turbulence can be suppressed. The cases of intermittent turbulence suggest that the global coordination is not an absolute one for intermediate noise intensities, and that the time needed for the active medium to recover plays a role in the alternation periodicity.

In the numerical simulations performed adding external noise to the KEE model, the effects of the fluctuations are qualitatively equivalent to the experimental case. Low noise does not modify the dynamics of the system and large noise eliminates turbulence for similar noise intensities. For intermediate noise intensities, alternation between global oscillations and complex dynamics are also observed mimicking the experimental results. The accuracy of the numerical simulations allows the observation of a richer phenomenology for these intermediate intensities. Moreover, other interesting patterns induced by the noise are also witnessed in the simulations, such as the formation of clusters or the generation of local pacemakers during several oscillations. Two examples of such small pacemakers in the same numerical simulation can be seen in Fig. 7, where the onset of the turbulence is delayed by the noise (too weak to completely suppress the turbulence) and two transitory pacemakers appear instead of the turbulence. Similar types of patterns have been previously observed in the same system under global feedback.[25]

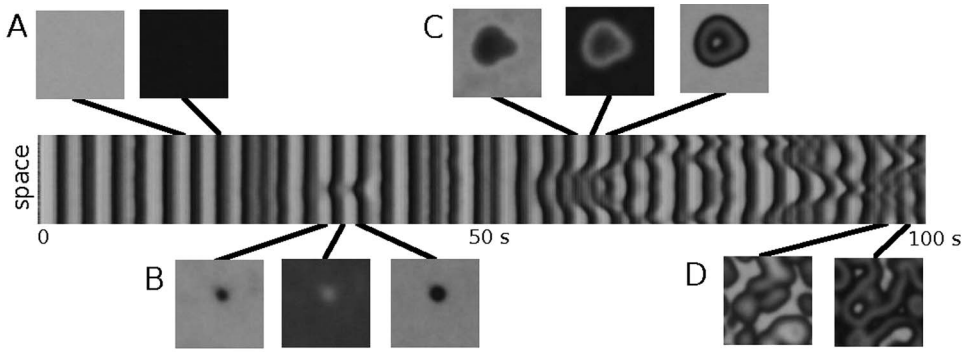

FIG. 7. Space-time plot of the evolution of the system under turbulent conditions and with external stochastic forcing. Snapshots of the system are plotted in the panels. Panel (a) shows the initial global oscillation typically observed in the numerical simulation. Panel (b) shows the growth of a single spot, which finally disappears. Panel (c) shows the generation of a pacemaker due to the intermediate amplitude of the external global noise. Panel (d) shows the turbulent patterns. Values of the partial pressures are $p_{O_2}=1.3\times10^{-4}$ and $p_{CO}=4.81\times10^{-5}$. Internal and external noises are $\epsilon_i=0.0005$ and $\sigma=0.3\%p_{CO}$, respectively. The size of the system is 0.2×0.2 mm^2.

The control of chemical turbulence has been previously studied with other techniques implying global resonant periodic forcing,[13] feedback mechanisms,[19] or local reaction modifications via microstructures or laser.[21] The forcing amplitude, percentage of CO partial pressure, needed to effectively suppress turbulent states was reported to be 10%–20% for the periodically forced reaction.[22] Closer analysis of the initial turbulent dynamics, determining the natural frequency of the system, and performing periodical global forcing at a resonant frequency[13] allows us to reduce that needed percentage in two orders of magnitude. As shown here, the same order of magnitude (0.1%–0.2%) is enough for fast random modulations to reach total entrainment. It is remarkable that the latter is independent of our previous knowledge of the system.

The intensities of the external noise that eliminates the turbulence in the numerical simulations are also quite low (0.2%–0.5%) and they are comparable to the case of resonant forcing.[31]

The fluctuations also have an influence on the transition between two stable states, anticipating a bistable transition of the system and shortening the intrinsic hysteresis loop. Using a mechanistic heuristic model, the bistable transition anticipation is conceptually equivalent to the motion of a particle localized in the higher minimum in a tilted double-well potential,[32] in which external noise adds energy to the system to save the potential barrier. For moderate noise, it has been shown that the reaction mechanism of the system more easily jumps the barrier that separates the two steady regimes. For large noise, this barrier would become so low in front of the fluctuations that the system would always be at one of the two local minima of the potential or transiting between them.

Defect-induced fronts were experimentally observed during the anticipated bistable transitions. When the transitions were completed and the crystal surface showed a full CO coverage, deep drops in the p_{CO} signal may lead to the emergence of spirals and target patterns at some defects of the surface. These oxygen structures propagated along the surface for a short time before they disappeared.

Besides the spatiotemporal noise-induced patterns, experiments performed with noise also featured an increase in the resulting amount of CO_2 produced in the CO oxidation. A mass spectrometer measured the CO_2 present in the UHV chamber while chemical turbulence developed, with and without modulating the p_{CO}. For the same amount of reactants involved in the reaction, integrated in time, the CO_2 production rate was higher with a fluctuating CO partial pressure. Higher productivity, thanks to fluctuating parameters, is a fact already observed in other environments, namely, the ozone production in atmospheres of urban areas.[32] This fact calls attention to the possible catalytic effect of noise, which might have some impact on the increase in chemical productivity for some other systems.

In the context of such real-world systems such as marine ecosystems[33,34] or ozone production,[32] in which stochasticity processes combine with periodic annual or daily cycles, it seems worthwhile for the future to combine the two global modifications: Periodic and noisy modulations of the CO oxidation reaction parameters.

In conclusion, we have shown that a stochastic external global signal introduced in the CO oxidation on Pt(110) through the partial pressure of the CO can eliminate spatiotemporal turbulence with low characteristic amplitudes of the noise, comparable and even smaller than in equivalent studies with the amplitudes of periodic forcing. Furthermore, this artificially noisy signal can anticipate phase transitions in bistable conditions by reducing the reaction intrinsic hysteresis loop.

ACKNOWLEDGMENTS

Financial support of the EU Marie Curie Research and Training Network "Unifying principles in nonequilibrium pattern formation" is gratefully acknowledged. S.A. also acknowledges support from the German Science Foundation (DFG) within the framework of Sonderforschungbereich 555 (SFB 555) "Complex nonlinear processes."

[1] R. Kapral and K. Showalter, *Chemical Waves and Patterns* (Kluwer, Dordrecht, 1995).
[2] A. S. Mikhailov and K. Showalter, Phys. Rep. **425**, 79 (2006).
[3] H. Haken, *Advanced Synergetics* (Springer, Berlin, 1985).
[4] G. Nicolis and I. Prigogine, *Self-Organization in Non-equilibrium Systems* (Wiley, New York, 1977).
[5] W. Horsthemke and R. Lefever, *Noise-Induced Transitions* (Springer, Berlin, 1984).
[6] F. Sagués, J. M. Sancho, and J. García-Ojalvo, Rev. Mod. Phys. **79**, 829 (2007).
[7] S. Kadar, J. C. Wang, and K. Showalter, Nature (London) **391**, 770 (1998).
[8] S. Alonso, I. Sendiña-Nadal, V. Pérez-Muñuzuri, J. M. Sancho, and F. Sagués, Phys. Rev. Lett. **87**, 078302 (2001).
[9] S. Alonso, D. G. Míguez, and F. Sagués, Europhys. Lett. **81**, 30006 (2008).
[10] I. Sendiña-Nadal, S. Alonso, V. Pérez-Muñuzuri, M. Gómez-Gesteira, V. Pérez-Villar, L. Ramírez-Piscina, J. Casademunt, J. M. Sancho, and F. Sagués, Phys. Rev. Lett. **84**, 2734 (2000).
[11] L. Q. Zhou, X. Jia, and Q. Ouyang, Phys. Rev. Lett. **88**, 138301 (2002).
[12] S. Jakubith, H. H. Rotermund, W. Engel, A. von Oertzen, and G. Ertl, Phys. Rev. Lett. **65**, 3013 (1990).
[13] P. S. Bodega, P. Kaira, C. Beta, D. Krefting, D. Bauer, B. Mirwald-Schulz, C. Punckt, and H. H. Rotermund, New J. Phys. **9**, 61 (2007).
[14] S. Wehner, P. Hoffmann, D. Schmeisser, H. R. Brand, and J. Küppers, Phys. Rev. Lett. **95**, 038301 (2005).
[15] P. Hoffmann, S. Wehner, D. Schmeisser, H. R. Brand, and J. Küuppers, Phys. Rev. E **73**, 056123 (2006).
[16] M. Pineda, R. Imbihl, L. Schimansky-Geier, and Ch. Zülicke, J. Chem. Phys. **124**, 044701 (2006).
[17] L. Yang, Z. Hou, and H. Xin, J. Chem. Phys. **109**, 2002 (1998).
[18] *Handbook of Chaos Control*, edited by E. Schöll and H. G. Schuster (Wiley-VCH, Weinheim, 1999).
[19] M. Bertram, C. Beta, M. Pollmann, A. S. Mikhailov, H. H. Rotermund, and G. Ertl, Phys. Rev. E **67**, 036208 (2003).
[20] C. Beta, M. Bertram, A. S. Mikhailov, H. H. Rotermund, and G. Ertl, Phys. Rev. E **67**, 046224 (2003).
[21] M. Stich, C. Punckt, C. Beta, and H. H. Rotermund, Philos. Trans. R. Soc. London, Ser. A **366**, 419 (2008).
[22] M. Bertram, C. Beta, H. H. Rotermund, and G. Ertl, J. Phys. Chem. B **107**, 9610 (2003).
[23] K. Krischer, M. Eiswirth, and G. Ertl, J. Chem. Phys. **96**, 9161 (1992).
[24] H. H. Rotermund, S. Nettesheim, A. von Oertzen, and G. Ertl, Surf. Sci. **275**, L645 (1992).
[25] M. Bertram, C. Beta, M. Pollmann, A. S. Mikhailov, H. H. Rotermund, and G. Ertl, Phys. Rev. E **67**, 036207 (2003).
[26] J. Wolff, M. Stich, C. Beta, and H. H. Rotermund, J. Phys. Chem. B **108**, 14282 (2004).
[27] M. Baer and M. Eiswirth, Phys. Rev. E **48**, R1635 (1993).
[28] J. García-Ojalvo and J. M. Sancho, *Noise in Spatially Extended Systems* (Springer, New York, 1999).

[29] C. Beta, A. S. Mikhailov, H. H. Rotermund, and G. Ertl, Europhys. Lett. **75**, 868 (2006).
[30] R. Imbihl and G. Ertl, Chem. Rev. (Washington, D.C.) **95**, 697 (1995).
[31] J. Davidsen, A. Mikhailov, and R. Kapral, Phys. Rev. E **72**, 046214 (2005).
[32] Z. H. Liu, Y. C. Lai, and J. M. Lopez, Chaos **12**, 417 (2002).
[33] J. E. Truscott and J. Brindley, Bull. Math. Biol. **56**, 981 (1994).
[34] C. S. Zhou and J. Kurths, New J. Phys. **7**, 18 (2005).